Comparative Evaluation of Salt Tolerance in Four Self-Rooted Hazelnut (*Corylus avellana* L. and *Corylus americana* Walter) Cultivars

Xavier Rius-Garcia [1,2], María Videgain-Marco [1,3], José Casanova-Gascón [1,3], Luis Acuña-Rello [4] and Pablo Martín-Ramos [4,*]

1 Department of Agricultural and Environmental Sciences, Higher Polytechnic School of Huesca, University of Zaragoza, Ctra. Cuarte s/n, 22071 Huesca, Spain; xrius@agromillora.com (X.R.-G.); mvidegain@unizar.es (M.V.-M.); jcasan@unizar.es (J.C.-G.)

2 Agromillora Group, Plaça Manel Raventós 3-5, St. Sadurní d'Anoia, 08770 Barcelona, Spain

3 AgriFood Institute of Aragón (IA2–CITA–University of Zaragoza), Ctra. Cuarte s/n, 22071 Huesca, Spain

4 Department of Agricultural and Forestry Engineering, ETSIIAA, University of Valladolid, Avda. Madrid 44, 34004 Palencia, Spain; luis.acuna@uva.es

* Correspondence: pmr@uva.es

Abstract: Rising soil salinity poses a significant challenge to hazelnut cultivation, particularly in Mediterranean regions, where the increasing use of low-quality irrigation water necessitates the identification of salt-tolerant cultivars for sustainable production. This study investigated the salt tolerance mechanisms in four hazelnut cultivars (Barcelona, Tonda di Giffoni, Tonda Gentile Romana, and Yamhill) exposed to varying NaCl concentrations (0, 25, 50, and 75 mM) over five months. This research assessed their morphological, physiological, and biochemical responses through an analysis of their growth parameters, photosynthetic efficiency, visual symptoms, and ion content. The results revealed significant genotypic variation in their salt tolerance mechanisms. Tonda di Giffoni demonstrated superior salt tolerance, maintaining a higher photosynthetic efficiency and better ion balance, particularly in K^+/Na^+ and Ca^{2+}/Na^+ ratios. Barcelona showed moderate tolerance at lower salinity levels but declined sharply under higher stress. Yamhill exhibited a strong survival capacity despite its poor photosynthetic performance, while Tonda Gentile Romana proved most sensitive to salinity stress. All the cultivars showed a significant biomass reduction, with their fresh and dry weights decreasing by over 80% at 75 mM NaCl. Leaf chloride concentrations dramatically increased, reaching levels 481% higher than those in the control conditions. This study identifies Tonda di Giffoni as the most suitable cultivar for moderately saline conditions and provides insights into hazelnut salt tolerance mechanisms, contributing valuable information for breeding programs and cultivation strategies in salt-affected regions.

Keywords: abiotic stress; ion homeostasis; photosynthetic efficiency; genetic variability; chlorophyll fluorescence; mineral content

1. Introduction

Hazelnut (*Corylus* spp.) stands as one of the most important and widely distributed nut species globally, thriving in regions characterized by mild, humid winters and cool summers. The main and traditional hazelnut-producing areas are located between the 40th and 45th latitude North, often near large water bodies such as the Black, Caspian, and Mediterranean seas. The states of Oregon and Washington in the USA are also a relevant

cultivation area [1]. Its significance extends beyond food production to applications in nutrition, human health, cosmetics, and pharmaceuticals [2].

Recently, hazelnut cultivation has been expanded in traditional producer countries and established in new places in the southern hemisphere, including Chile, South Africa, and Australia. Introducing hazelnuts into new environments can reduce their productivity, lead the trees to experience eco-physiological disorders, and expose the crop to high pressure from common and new pests and diseases [1]. Further, the impacts of climate change may significantly affect the global hazelnut market depending on production and yield changes [3,4]. Hence, approaches in cultivar and rootstock choice guidance are required to improve the adaptability of hazelnuts to biotic and abiotic stresses [5].

Historical selection of hazelnut genotypes has resulted in varieties adapted to specific environmental conditions, including air temperature and humidity levels [6–8]. Within *Corylus avellana* L., notable European cultivars include Tonda Gentile and Tonda Gentile Romana from central Italy and Tonda di Giffoni from southern Italy, which show varying degrees of adaptability when cultivated outside their native environments [2,9]. Similarly, specific local *C. avellana* genotypes in Karaj, Iran, were selected as rootstocks due to their tolerance to drought and low humidity [10]. *Corylus americana* Walter, native to North America, has also contributed important cultivars to commercial production. Two notable examples are Yamhill, which exhibits high yields and adaptability across diverse environments [11], and Barcelona, known for its nut size and quality [12].

Irrigation plays a crucial role in hazelnut cultivation, particularly in areas with limited rainfall and soils with a poor water-holding capacity [13]. Hazelnuts are considered sensitive to water stress due to their limited stomatal regulation capability [14–17] and their typically shallow root system [18]. Water scarcity presents a significant challenge to hazelnut production in the Mediterranean region, where supplemental irrigation is often necessary during late spring and early summer. This period is critical for photosynthate production, supporting both fruit development and reserve accumulation for the subsequent year [2,15,19].

The challenge of water scarcity extends far beyond the Mediterranean basin, representing a global threat to agricultural sustainability [20]. Growing demands from domestic and industrial sectors strain agricultural water supplies and contribute to groundwater depletion [21,22]. Consequently, many countries are exploring the use of lower-quality water sources (brackish, reclaimed, drainage) with higher salinity levels to address water shortages and maintain agricultural development [23]. This trend is particularly evident in major agricultural regions worldwide—in Central Asia, over 50% of irrigated lands face challenges with saline water use [24], while similar issues affect agricultural production in North America, Australia, and parts of China and Iran.

The increasing reliance on saline water for irrigation, combined with existing soil salinity problems, poses a significant threat to agricultural productivity. Currently, soil salinity affects approximately 831 million hectares worldwide [25], with China (211.74 million hectares), Kazakhstan (93.31 million hectares), and Iran (88.33 million hectares) facing the most extensive challenges [26]. The USA also experiences significant salinization, primarily in irrigated lands across arid and semi-arid regions, while Australia faces unique challenges, with 2.5 million hectares affected by dryland salinity [26]. These issues are projected to intensify, with estimates suggesting that half of all arable land globally will be impacted by salinity by 2050 [25].

For hazelnut cultivation, these trends present particular challenges due to the crop's specific sensitivities. Excessive salinity can trigger a range of adverse effects, with ionic imbalance being one of the primary consequences. High concentrations of sodium and chloride ions initiate detrimental biochemical reactions that can lead to plant death [27,28].

Furthermore, sodium and chloride toxicity impairs nutrient uptake and induces physiological drought by lowering the osmotic potential of soil solutions [29]. The impact extends to all aspects of photosynthesis, altering the overall condition of this process in stressed plants [30,31].

Despite the growing concern about salinization in traditional hazelnut-growing regions, research on salt tolerance in *Corylus* species remains limited compared to that in other tree crops. While recent studies have begun to address this knowledge gap—with Porghahreman et al. [32] investigating the short-term (12 weeks) responses of European cultivars (Segorb, Ronde de Piemant, Fertile de Coutard, and Negret) to salinity stress and Luo et al. [33] examining the ion transport mechanisms in a Ping'ou hybrid hazelnut—, comprehensive evaluations of the salt tolerance mechanisms across different *Corylus* species and cultivars remain scarce. Previous research has primarily focused on individual physiological responses, particularly to water stress, but longer-term analyses integrating multiple stress response parameters are lacking.

This study aimed to compare the responses of four self-rooted hazelnut cultivars—two *C. avellana* cultivars (Tonda di Giffoni and Tonda Gentile Romana) and two *C. americana* cultivars (Yamhill and Barcelona)—to varying levels of saline water over five months. The goal was to elucidate the morphological, physiological, and biochemical mechanisms involved in their salt tolerance. Understanding these mechanisms and identifying their salinity thresholds have direct practical implications for the hazelnut industry. These findings could guide cultivar selection in regions facing increasing soil salinization and inform the development of irrigation management strategies in areas using low-quality water. Additionally, the identification of salt-tolerant traits may establish screening criteria for breeding programs targeting enhanced salinity tolerance while also enabling risk assessments for existing orchards experiencing salinization issues. This investigation, conducted under controlled conditions, assessed the NaCl tolerance of these cultivars, ranking them according to their resilience to salt stress and determining the threshold salinity levels at which they exhibited stress symptoms, thereby providing evidence-based guidelines for sustainable hazelnut cultivation in salt-affected areas.

2. Materials and Methods

2.1. Experimental Setup and Plant Material

This experiment was conducted in a polyethylene greenhouse at the Escuela Politécnica Superior, Universidad de Zaragoza, in Huesca, Spain (42°07′12.78″ N, 0°26′49.04″ W). In June 2022, uniform 12-month-old plants from four self-rooted hazelnut genotypes (Tonda di Giffoni, Tonda Gentile Romana, Yamhill, Barcelona) were obtained from Agromillora Iberia nursery (Subirats, Barcelona, Spain). The plants were transplanted into black plastic pots (15 × 15 × 20 cm, 4.5 L) filled with quartziferous sand (0.05–2.00 mm). During transplantation, the roots were rinsed with deionized water to remove residual peat.

The plants were grown for seven months and pruned to a height of 60 cm in January 2023. The experiment began on June 1st, when the new main shoot reached a height of 50 cm, and continued for five months, concluding on 1 November 2023. The plants were maintained under natural light conditions in the greenhouse, with the daily temperatures ranging from 18 to 33 °C and the relative humidity varying between 55% and 85%. An automatic mobile screen, activated at 27 °C, reduced the daytime temperatures, while a ventilation system ensured that the internal air temperature remained below 35 °C.

The experimental design followed a completely randomized block format with 64 self-rooted hazelnut plants, comprising four plants per treatment (four salinity levels) and cultivar (four) combinations.

Plant responses were monitored through biweekly visual assessments of four plants per treatment.

2.2. Irrigation Treatment and Management

Plants were irrigated with a 1/4 strength Hoagland solution [34] prepared with local fresh water (electrical conductivity: 0.8 dS m^{-1}). The four genotypes were subjected to four salt levels (0, 25, 50, and 75 mM NaCl) over a five-month period, with the salt concentrations increased by 25 mM NaCl weekly until the target levels were reached, starting on 1 June.

The selected salinity concentrations (0, 25, 50, and 75 mM NaCl) were chosen to represent both current and projected irrigation quality challenges in agricultural systems. The 25 and 50 mM NaCl treatments reflect typical salinity ranges when using brackish water for irrigation, while the 75 mM NaCl treatment was included to evaluate the cultivars' responses under extreme stress conditions, clearly differentiate genotypic tolerance thresholds, and anticipate the worst-case scenarios under projected climate change impacts. This range of concentrations ensures practical relevance while facilitating clear differentiation of cultivar-specific tolerance mechanisms. Our selected concentrations also align with recent hazelnut salinity studies (e.g., Porghahreman et al. [32], using 0–90 mM NaCl gradients), enabling meaningful comparisons across the research.

The irrigation frequency and duration varied according to the weather conditions, with 4-min sessions conducted one to three times daily. Each pot was equipped with two drippers, with each delivering a flow rate of 1.3 L h^{-1} (Click Tip HD, Naandanjain, Jalgaon, India). Saline solutions were injected into the irrigation system using a MixRite E-300 volumetric pump (Tefen Flow and Dosing Technologies Ltd., Kibbutz Farod, Israel), and irrigation scheduling was managed using an Agronic 5500 irrigation controller (Sistemes Electrònics PROGRÉS, Barcelona, Spain).

The irrigation water exhibited electrical conductivity (EC$_{iw}$) and sodium adsorption ratio (SAR$_{iw}$) levels of 0.8, 3.0, 6.0, and 9.0 dS m^{-1} and 2, 30, 60, and 90, respectively, with the pH values ranging from 7.2 to 7.4. Weekly electrical conductivity measurements of the drainage water using a Hanna Instruments-HI 9033 conductimeter (Woonsocket, RI, USA) yielded values of 0.8, 3.2, 6.1, and 9.2 dS m^{-1} corresponding to the 0, 25, 50, and 75 mM NaCl concentrations. A leaching fraction of 20–30% was maintained during irrigation to ensure consistent salinity levels in the pots throughout the experiment [35]. This leaching fraction was maintained through systematic monitoring of the drainage water. The experimental setup included pots arranged on an inclined table (2% slope) with waterproof plastic sheeting, allowing for complete drainage collection. The drainage water EC values consistently matched the expected levels throughout the experiment: 0.8, 3.2, 6.1, and 9.2 dS m^{-1} for the control, 25, 50, and 75 mM NaCl concentrations.

2.3. Biomass Measurements

At the conclusion of the experiment, the plants were harvested and separated into roots, wood, stems, and leaves. Aerial parts were washed with distilled water, while roots were cleaned with deionized water. Their fresh weights were recorded immediately (except for totally necrosed leaves), and the samples were then dried at 70 °C for 24 h to determine their dry weights.

2.4. Mineral Content Analysis

The dried plant materials were ground into particles smaller than 2 mm using an electrical grain grinder (CGoldenwall model HC400, Wuxi, China). The analysis employed both wet chemistry methods and a Niton XL3t GOLDD+ portable X-ray fluorescence (pXRF) spectrometer (Thermo Scientific, Waltham, MA, USA). The <2 mm particle size was

selected to simulate processed soil sample conditions suitable for measurement with the pXRF probe, following the established protocols [36–38].

The pXRF instrument measured the Ca^{2+}, K^+, and Cl^- concentrations without pretreatment, using the 'Soil mode' for Ca^{2+} and K^+ and the 'Mining mode' for Cl^- [39,40]. The pXRF instrument's internal calibration was conducted at Thermo Fisher Messtechnik GmbH (Munich, Germany). The method validation employed a parallel analysis with the conventional techniques. For Ca^{2+} and K^+, atomic absorption spectrometry served as the reference method, while the Cl^- measurements were validated through ion chromatography in an accredited laboratory (Eurofins Scientific, Lleida, Spain). The correlations between the pXRF and reference methods showed strong linear relationships ($R^2 > 0.95$ for all analytes). Quality control measures included a regular check standard analysis, daily instrument verification, blank measurements, duplicate analyses, and standardized sample preparation protocols.

For the sodium analysis, the dried and ground samples underwent nitric acid digestion. Approximately 0.5 g of sample material was predigested with 10 mL of trace metal-grade HNO_3 for 1 h, followed by heating to 115 °C for 2 h and subsequent dilution to 50 mL with deionized water [41]. The sodium content was determined using atomic absorption spectrometry (SpectrAA 10, Varian, CA, USA) following the methodology described by Kalra [42]. All of the reported values represent the averages of four replicate measurements.

The combined use of the pXRF and wet chemistry methods optimized both efficiency and accuracy in our elemental analysis. pXRF enabled rapid, non-destructive analysis of Ca^{2+}, K^+, and Cl^- with minimal sample preparation, allowing for efficient processing of our large sample set. However, recognizing pXRF's limitations for light elements, we incorporated atomic absorption spectrometry for Na^+ quantification, which provided superior sensitivity and established reliability for this critical ion. This complementary approach ensured both high-throughput screening and precise quantification of all the target elements while maintaining cost-effectiveness.

2.5. Physiological Measurements

Chlorophyll fluorescence parameters were recorded biweekly using a portable Handy PEA fluorimeter (Hansatech Instruments Ltd., Norfolk, UK). The measurements included initial fluorescence (F_0), maximum fluorescence (F_m), variable fluorescence ($F_v = F_m - F_0$), and the maximum quantum yield of photosystem II (PSII) (F_v/F_m) in the dark-adapted leaves. These parameters were grouped into three categories: overall efficiency of photosystem II, energy and electron transport, and energy dissipation and damage [43–45].

2.6. Statistical Analysis

All of the statistical analyses were performed using R software (v. 4.4.1:2024) [46]. The experimental design comprised a complete 3-factor factorial arrangement (genotype, treatment, and organ) with 4 levels each and 4 replicates, totaling $4^3 \times 4 = 256$ trials. The analysis focused on Ca^{2+}, Na^+, K^+, Cl^-, wet weight, dry weight, and key ionic ratios (Ca^{2+}/Na^+ and K^+/Na^+).

The statistical approach was guided by a systematic data assessment. Initial testing revealed significant deviations from normality in the ion concentration and biomass data, confirmed through the Kolmogorov–Smirnov test with Lilliefors correction [47] or the Shapiro–Wilk test [48], depending on sample size, with Q-Q normal probability plots providing visual validation. Homoscedasticity was evaluated using Levene's test [49]. Given the frequent violations of normality and homoscedasticity assumptions, two alternative statistical approaches were employed: the Kruskal –Wallis test [50] for non-normal but homoscedastic groups and Welch's heteroscedastic F test with trimmed means and Win-

sorized variances [51,52] when neither normality nor homoscedasticity could be assumed. Bootstrap methods were utilized to establish robust confidence intervals for location and homogeneous groups [53], as this methodology offered reliable quantification of uncertainty given the non-normal distribution and heteroscedastic nature of our dataset across the treatments. This approach was particularly suitable for our factorial design examining genotype, treatment, and organ interactions. The statistical framework chosen ensured a robust analysis of the stress response data while maintaining statistical rigor without relying on potentially violated parametric assumptions.

The survival analysis was conducted using the Kaplan–Meier Product-Limit estimator.

3. Results

3.1. Biomass Production Response to Salinity Stress

3.1.1. Fresh Weight Response to Salinity Stress

Analysis of the genotypic responses revealed that under the control conditions, Barcelona and Tonda di Giffoni exhibited the highest fresh weights of 65.51 g and 67.01 g, respectively, while Tonda Gentile Romana and Yamhill showed lower values of 38.11 g and 34.88 g (Table S1 and Figure S1). When exposed to 25 mM NaCl, all genotypes experienced substantial reductions in fresh weight: Barcelona decreased to 24.56 g, Yamhill to 22.72 g, and Tonda Gentile Romana showed the most severe reduction, down to 14.03 g. At 50 mM NaCl, the fresh weights ranged from 12.52 g in Barcelona to 13.41 g in Yamhill. Under the highest salinity (75 mM NaCl), Barcelona and Tonda Gentile Romana recorded the lowest fresh weights (7.23 g and 7.53 g, respectively), while Tonda di Giffoni and Yamhill maintained relatively higher values (12.79 g and 9.75 g, respectively).

The distribution of fresh weight across the plant organs showed that in the control plants, the stems exhibited the highest fresh weight (77.75 g), followed by the leaves (52.46 g), roots (45.86 g), and wood (29.44 g). Salinity stress progressively reduced the fresh weight across all organs (Table S2 and Figure S2). At 25 mM NaCl, roots maintained a higher fresh weight (25.98 g) compared to that of the stems (22.66 g) and leaves (13.07 g). At higher salinity levels (50 and 75 mM NaCl), the roots and wood demonstrated greater resilience, maintaining fresh weights of 16.65 g and 15.52 g at 50 mM NaCl and 11.48 g and 12.13 g at 75 mM NaCl. The stems showed the most dramatic reduction, decreasing to 7.01 g at 50 mM NaCl and 4.69 g at 75 mM NaCl.

3.1.2. Dry Weight Response to Salinity Stress

Examination of the dry weight patterns showed that under the control conditions, Tonda di Giffoni demonstrated the highest dry weight (38.02 g), followed by Barcelona (32.41 g), Tonda Gentile Romana (21.53 g), and Yamhill (17.69 g). At 25 mM NaCl (Table S3 and Figure S3), Barcelona and Tonda di Giffoni showed similar reductions (11.83 g and 11.87 g), while Tonda Gentile Romana exhibited the lowest dry weight (6.94 g). At 50 mM NaCl, Tonda di Giffoni maintained a slightly higher dry weight (8.58 g), while the other cultivars ranged from 6.08 g to 6.71 g. At the highest salinity level (75 mM NaCl), Tonda di Giffoni retained the highest dry weight (6.93 g), while the other cultivars showed more severe reductions (Barcelona: 3.87 g; Tonda Gentile Romana: 4.48 g; Yamhill: 5.04 g).

The partitioning of the dry matter in the control plants revealed the highest accumulation in the stems (41.59 g), followed by the roots (27.81 g), leaves (22.66 g), and wood (17.60 g). The addition of NaCl caused substantial dry weight reductions in all plant parts (Table S4 and Figure S4). In the 25 mM NaCl treatment, the hierarchy of dry matter accumulation shifted: the roots became the dominant sink (12.42 g), closely followed by the wood (11.66 g) and stems (11.19 g), while the leaves showed a marked reduction (7.01 g). More severe salt stress led to further tissue-specific responses. At 50 mM NaCl, the wood

and roots demonstrated similar dry weights (8.85 g and 8.36 g, respectively), in contrast to the pronounced decline observed in the stems (3.37 g). The most extreme treatment (75 mM NaCl) revealed differential tissue sensitivity, with the roots and wood maintaining moderate dry weights (7.11 g and 6.29 g), while the stem tissue showed the greatest susceptibility (2.03 g).

3.2. Physiological Responses to Salinity Stress

3.2.1. Temporal Changes in Photochemical Efficiency

The initial measurements in April under control conditions established the baseline physiological performance for all cultivars (Figure 1, Table S5). The chlorophyll fluorescence parameters highlighted the temporal progression of the salt stress effects throughout the experiment. The measurements taken in June revealed immediate stress responses, particularly under the 50 and 75 mM NaCl treatments, characterized by reduced photochemical efficiency across cultivars, with the exception of Tonda di Giffoni. By September, the data reflected longer-term adaptation patterns, showing cultivar-specific responses: Tonda di Giffoni maintained relatively stable photosynthetic parameters, whereas the other cultivars exhibited varying degrees of physiological decline. This temporal analysis provided a foundational framework for understanding the specific responses detailed in subsequent sections.
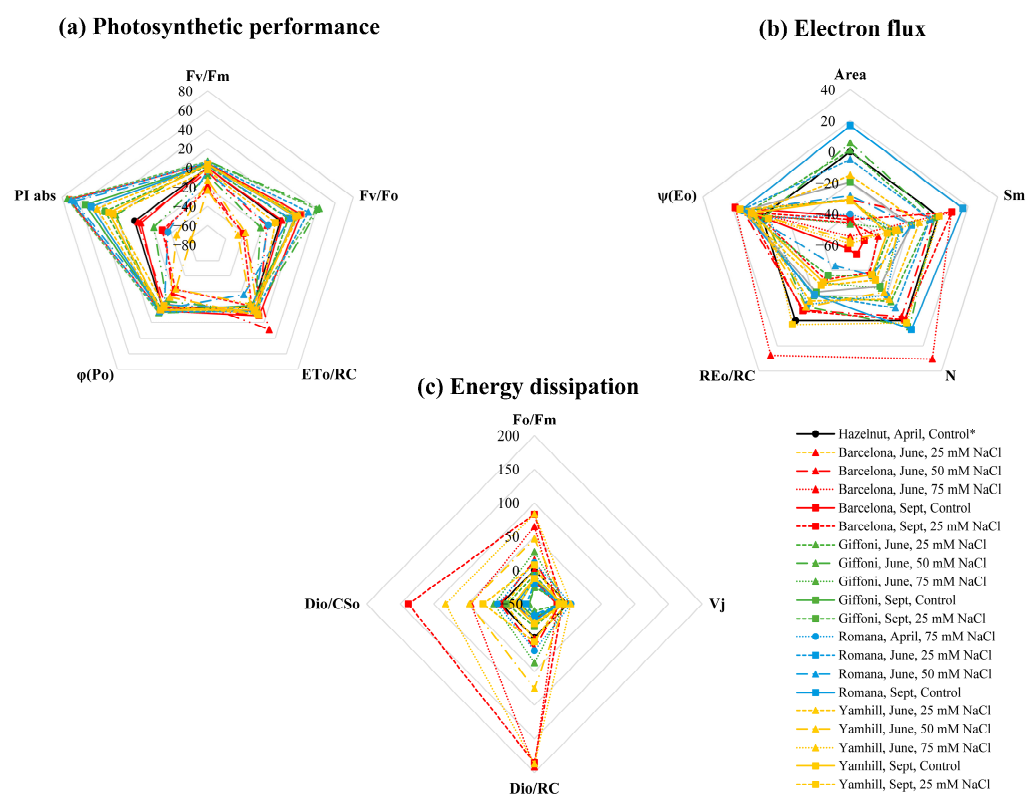
Figure 1. Photosynthetic parameters of hazelnut cultivars under varying salinity levels at the conclusion of the experiment. (**a**) Photosynthetic performance, (**b**) energy dissipation, and (**c**) electron flux. 'Hazelnut, April, Control*' represents average values across all genotypes in April. Parameters shown include Area (electron acceptor pool size), F_v/F_m (maximum PSII quantum efficiency), Vj (primary quinone electron acceptor reduction state), Sm (normalized complementary area above OJIP transient), N (QA turnover number), DIo/RC (energy dissipation per reaction center), ETo/RC (electron transport rate per reaction center), REo/RC (electron transport rate beyond QA), φ(Po) (primary photochemistry quantum yield), ψ(Eo) (trapped exciton movement efficiency), DIo/CSo (energy dissipation per cross-section), and PI_abs (performance index on absorption basis).

3.2.2. Photosynthetic Performance

Tonda di Giffoni demonstrated the highest salt tolerance among all cultivars (Figure 1a), maintaining positive performance index values on an absorption basis (PI_abs) throughout the study period, ranging from 54.33 in the control conditions to 20.88 at 50 mM NaCl. Barcelona exhibited a satisfactory performance under low salinity, with a PI_abs value of 71.86 in control conditions, but showed a sharp decline to -33.23 at 75 mM NaCl. Yamhill exhibited the lowest salt tolerance, with severe reductions in its photosynthetic efficiency, declining from 28.49 in control conditions to -61.62 at 75 mM NaCl. Tonda Gentile Romana displayed moderate tolerance but experienced significant declines under higher salinity levels.

3.2.3. Electron Transport Chain Response

All of the cultivars showed disruption in their electron transport chain, though with varying degrees of severity (Figure 1b). Tonda di Giffoni maintained the most stable electron flow under moderate salinity conditions. Barcelona showed inconsistent patterns, with negative electron transport rate per reaction center (REo/RC) values (-57.41) even at low salinity. Yamhill displayed significant fluctuations in electron flow, ranging from negative to positive values (82.39 at 75 mM NaCl). Tonda Gentile Romana consistently demonstrated negative electron flow across all salinity levels, indicating a consistent disruption in its electron transport system.

3.2.4. Energy Dissipation Patterns

Barcelona and Yamhill exhibited the highest energy dissipation rates (Figure 1c), with energy dissipation in the form of heat and fluorescence per reaction center (Dio/RC) reaching values around 185–187 under the control conditions. These rates suggest significant stress even at lower salinity levels. Tonda Gentile Romana showed moderate energy dissipation, with DIo/RC values around -25.45 under control conditions. In contrast, Tonda di Giffoni demonstrated the most efficient energy utilization, maintaining consistently lower dissipation rates across all salinity levels.

3.3. Visual Symptoms and Survival Analysis

3.3.1. Progressive Stress Response

Under the control conditions, all genotypes exhibited vigorous growth characterized by healthy green leaves, upright stems, and well-developed root systems (Figure 2a).

At 25 mM NaCl, genotype-specific responses emerged: Barcelona maintained relatively healthy leaves with minimal stress symptoms, while Tonda Gentile Romana showed early signs of wilting. Tonda di Giffoni retained most of its foliage, showing only mild discoloration, whereas Yamhill displayed more pronounced leaf yellowing. The root systems remained largely intact across all genotypes, although Yamhill showed a slight reduction in root density.

At 50 mM NaCl, the stress impacts intensified significantly. Barcelona and Tonda di Giffoni showed leaf browning and partial defoliation, with Barcelona retaining a comparatively greater proportion of its foliage. Tonda Gentile Romana exhibited significant defoliation and stem decline, while Yamhill experienced near-complete leaf loss and severe stem dieback. The root mass decreased across all genotypes, though Barcelona and Tonda di Giffoni maintained denser root systems compared to Tonda Gentile Romana and Yamhill.

Severe stress symptoms were observed at 75 mM NaCl across all genotypes. The plants exhibited complete defoliation and extensive stem dieback. Their root systems showed a severe reduction; however, Barcelona and Tonda di Giffoni retained some structural

integrity. In contrast, Tonda Gentile Romana and Yamhill displayed near-total collapse of both their stems and roots, indicating their limited capacity to tolerate high salinity.

Figure 2. Visual assessment of salinity stress effects on hazelnut cultivars at the conclusion of the experiment, after five months of treatment. (**a**) Representative plants showing progressive stress symptoms from control (0 mM NaCl) to severe stress (75 mM NaCl) for each cultivar. (**b**) Root system morphology comparison among genotypes under severe salt stress (75 mM NaCl), highlighting architectural differences in stress adaptation. One replicate per treatment is shown.

The progression of visual symptoms followed distinct temporal patterns. At 25 mM NaCl, symptoms developed gradually over several weeks, while at 75 mM NaCl, the deterioration was more rapid. The images in Figure 2 represent the end-point conditions; however, the plant responses evolved progressively, with considerable variation in their timing and severity among cultivars.

Concerning root system response, the root architecture analysis revealed distinct genotypic differences in stress adaptation (Figure 2b). Yamhill developed extensive vertical root growth, in contrast to Tonda Gentile Romana's more compact root system. This difference suggests that Yamhill may possess superior salt partitioning capabilities, with its longer root system potentially facilitating stress mitigation by sequestering excess Na^+ in the lower roots, away from shoots. Tonda di Giffoni displayed a denser root mass compared to Barcelona, indicating a higher capacity to withstand the 75 mM NaCl stress,

possibly through more efficient ion exclusion mechanisms and enhanced K^+/Na^+ selectivity. Barcelona, with its moderately deep root system and balanced lateral development, represented an intermediate level of adaptation to salinity stress.

3.3.2. Survival Analysis

Leaf damage symptoms became apparent during the fourth fortnight and persisted until the conclusion of the experiment. The initial symptoms progressed from necrotic spots forming around the leaf edges to complete leaf death and defoliation.

The survival analysis revealed distinct genotypic responses to salinity stress (Figure 3). At 25 mM NaCl, all of the cultivars survived throughout the entire experimental period. Differences in survival emerged at 50 mM NaCl, where Tonda di Giffoni and Yamhill maintained viability for the entire experiment, while Barcelona showed lower survival (nine fortnights), and Tonda Gentile Romana exhibited the lowest survival rate (eight fortnights). Under severe stress (75 mM NaCl), all cultivars succumbed simultaneously at the eighth fortnight.
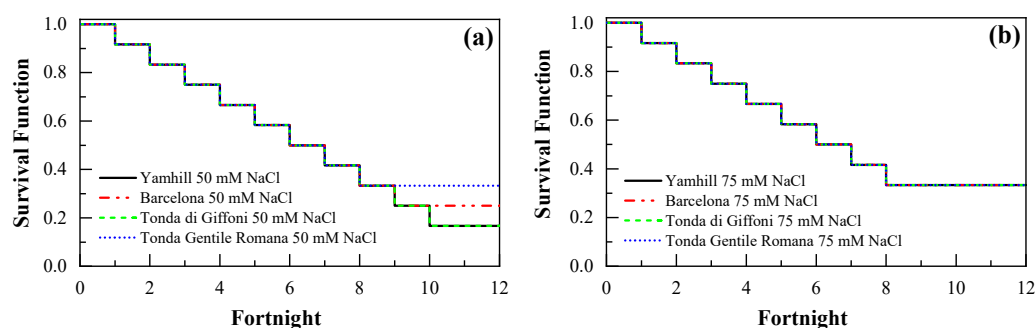

Figure 3. Survival plot for different genotypes under the two highest salinity treatments: (**a**) 50 mM NaCl and (**b**) 75 mM NaCl.

These survival patterns establish clear physiological thresholds: 25 mM NaCl represents a manageable stress level, 50 mM NaCl serves as a discriminating concentration revealing genotypic differences in tolerance, and 75 mM NaCl exceeds the adaptive capacity of all of the cultivars studied.

3.4. Mineral Content and Ion Relations

3.4.1. The Statistical Approach

Due to significant deviations from normality in the dataset (Table S6), logarithmic transformations were applied to the dependent variables to construct a general factorial model for ANOVAs. The model structure was defined as follows:

$$\log(\text{Dependent variable}) \sim \text{fact.A(Genotype)} \times \text{fact.B(Treatment)} \times \text{fact.C(Organ)}$$

All three factors (genotype, treatment, and organ) were statistically significant across all models (Table S7). Due to substantial heteroscedasticity and non-normality issues, robust comparison methods were employed using untransformed variables.

3.4.2. Calcium Dynamics

Under the control conditions, all genotypes showed similar calcium concentrations, averaging at 4.30% (Table S8 and Figure S5). Exposure to 25 mM NaCl resulted in genotype-specific reductions: Barcelona's concentration decreased by 25.7% to 3.26%, Tonda di Giffoni's by 14.3% to 3.71%, Tonda Gentile Romana's by 30.9% to 2.99%, and Yamhill's by 17.6% to 3.38%.

At 50 mM NaCl, the reductions in the calcium concentration became more pronounced. Barcelona experienced a 27% decrease to 2.38%, while Tonda di Giffoni showed a more modest decline from 7.9% to 3.42%. Tonda Gentile Romana and Yamhill decreased in calcium concentration by 14.4% and 16.9%, reaching concentrations of 2.56% and 2.81%, respectively. At the highest salinity level (75 mM NaCl), the final calcium concentrations stabilized at relatively low levels: Barcelona showed a 45.5% overall reduction to 2.40%, Tonda di Giffoni declined by 33.3% to 2.91%, and Tonda Gentile Romana and Yamhill demonstrated reductions of 38.3% and 43.4%, reaching final concentrations of 2.67% and 2.32%, respectively.

The organ-specific analysis revealed distinct calcium distribution patterns (Table S9 and Figure S6). Under the control conditions, the roots maintained the highest calcium concentration (8.22%), followed by the leaves (4.43%), stems (2.33%), and wood (2.18%). Salinity stress led to marked decreases in the calcium concentration within specific organs. At 25 mM NaCl, the root calcium levels fell by 30.3% to 5.73%, while the leaf concentrations decreased by 36.4% to 2.82%. The stems and wood displayed lower reductions, stabilizing at 2.99% and 1.81%, respectively. At 75 mM NaCl, the stems and wood reached their lowest calcium concentrations, declining to 1.57% and 0.89%, respectively, representing reductions of 46.8% and 59.2% relative to the control levels. The root calcium concentrations showed a slight recovery at this salinity level, increasing to 4.97%.

3.4.3. Potassium Distribution

The baseline potassium concentrations under the control conditions varied among genotypes (Table S10 and Figure S7): Tonda di Giffoni exhibited the highest level (2.88%), followed by Barcelona (2.65%), Tonda Gentile Romana (2.54%), and Yamhill (2.40%). The 25 mM NaCl treatment induced significant reductions in the potassium levels across all genotypes. Barcelona showed a 21.80% decrease to 2.07%, while Tonda di Giffoni experienced a smaller decline of 17.30% to 2.38%. Tonda Gentile Romana exhibited a 22.00% reduction to 1.98%, and Yamhill displayed the smallest reduction at this level, declining by 13.3% to 2.08%.

The potassium levels continued to decrease under the 50 mM NaCl treatment. Barcelona and Tonda di Giffoni decreased to 1.80% and 1.86%, respectively, representing reductions of 13.20% and 21.80% from the 25 mM NaCl level. Tonda Gentile Romana showed a more substantial reduction of 19.60% to 1.59%. Interestingly, Yamhill maintained a relatively stable potassium concentration of 2.00%, showing only a slight 4.00% decline.

At 75 mM NaCl, the potassium concentrations reached their lowest levels across all genotypes. Barcelona exhibited the most substantial reduction, with a 50.70% total decline from the control conditions to 1.31%. Tonda di Giffoni and Tonda Gentile Romana showed similar reductions, dropping by 49.00% and 48% to final concentrations of 1.47% and 1.32%, respectively. Yamhill demonstrated the lowest overall decline, maintaining 1.57%, representing a 34.60% reduction.

The organ-specific potassium distribution showed marked variation (Table S11 and Figure S8). Under the control conditions, the leaves contained the highest concentration (5.86%), followed by the stems (2.15%), roots (1.78%), and wood (0.68%). At 25 mM NaCl, leaf potassium remained relatively stable (5.84%), while the roots experienced a significant 45.30% reduction to 0.98%. In the stems and wood, it declined to 1.39% and 0.31%. The 50 mM NaCl treatment reduced leaf potassium by 13.9% to 5.03%, while the root levels dropped to 0.64%. At 75 mM NaCl, the leaves retained 4.29% potassium (26.80% reduction from the control), while the roots, stems, and wood showed the lowest concentrations (0.44%, 0.72%, and 0.22%), representing reductions of 75.40%, 66.70%, and 67.10% from the control values.

3.4.4. Chloride Accumulation

Under the control conditions, the chloride concentrations were relatively low across all genotypes (Table S12 and Figure S9): Barcelona (0.32%), Tonda di Giffoni (0.35%), Tonda Gentile Romana (0.28%), and Yamhill (0.34%). The 25 mM NaCl treatment triggered substantial increases: Barcelona showed a 276% increase, reaching 1.21%, while Tonda di Giffoni increased 171% to 0.95%. Tonda Gentile Romana and Yamhill showed more substantial increases of 353% and 233%, reaching 1.26% and 1.13%, respectively.

At 50 mM NaCl, the chloride levels continued to rise: Barcelona increased 45.4% from the 25 mM level, reaching 1.76%, while Tonda di Giffoni increased by 25.8% to 1.19%. Tonda Gentile Romana and Yamhill increased by 46.8% and 52.3% to 1.85% and 1.72%. The 75 mM NaCl treatment resulted in the highest chloride concentrations across all genotypes. Barcelona and Yamhill reached 1.87% and 2.09% (6.3 and 21.4% increases from 50 mM), while Tonda di Giffoni showed the smallest increase to 1.34%. Tonda Gentile Romana recorded the highest final concentration of 2.09%, representing a 13% increase from 50 mM NaCl.

The organ-specific analysis showed distinct chloride distribution patterns (Table S13 and Figure S10). The control leaves contained the highest concentration (0.88%), while the roots, stems, and wood showed lower levels (0.21%, 0.11%, and 0.09%). The 25 mM NaCl treatment increased the leaf chloride dramatically to 3.45% (a 289% increase), with chloride in the roots rising to 0.44% and reaching 0.41% and 0.25% in the stems and wood. At 75 mM NaCl, the leaves maintained 3.57%, while the roots and stems accumulated 0.75% and 2.24%, representing 22.4% and 47.4% increases from the 50 mM levels.

3.4.5. Sodium Distribution

Under the control conditions, the sodium levels were minimal across all genotypes (Table S14 and Figure S11): Barcelona (0.17%), Tonda di Giffoni (0.22%), Tonda Gentile Romana (0.16%), and Yamhill (0.16%). The 25 mM NaCl treatment induced significant increases in the sodium concentrations, with these rising to 0.70% and 0.72% in Barcelona and Tonda Gentile Romana (an approximately 300% increase). Yamhill increased its sodium concentrations to 0.67%, while Tonda di Giffoni showed a more moderate rise to 0.33%.

At 50 mM NaCl, Tonda Gentile Romana reached the highest concentration (1.11%, a 53% increase from the 25 mM level), while Barcelona and Yamhill showed similar values (0.94%, representing increases of 34% and 41%). Tonda di Giffoni maintained the lowest sodium concentration (0.72%, a 120% increase from the control). The 75 mM NaCl treatment resulted in peak sodium levels: Tonda Gentile Romana and Yamhill reached 1.38% and 1.37%, and Barcelona increased to 1.33% (a 41% rise from 50 mM), while Tonda di Giffoni, though it showed the lowest concentration, rose to 0.99%.

Under the control conditions, the sodium concentrations were minimal in all plant organs (Table S15 and Figure S12): the leaves (0.16%), roots (0.33%), stems (0.12%), and wood (0.10%). At 25 mM NaCl, leaf sodium increased dramatically to 1.15% (a 614% rise), while the sodium in the roots, stems, and wood increased to 0.66%, 0.33%, and 0.28%. The 50 mM NaCl treatment further increased the leaf sodium to 1.33%, with the root and stem sodium reaching 0.92% and 0.91%. At 75 mM NaCl, the leaves showed the highest concentration (2.25%, a 69.2% increase from 50 mM), while the roots and stems reached 1.17% and 0.78%, and wood increased to 0.87%.

3.4.6. The Potassium/Sodium Ratio

Under the control conditions, all genotypes showed high K^+/Na^+ ratios, indicating efficient potassium uptake and sodium exclusion (Table S16 and Figure S13): 17.66, 17.68, 17.40, and 15.05 for Barcelona, Tonda Gentile Romana, Yamhill, and Tonda di Giffoni,

respectively. However, following the NaCl treatments, these ratios were significantly reduced across all genotypes, highlighting the impact of salinity stress. At 25 mM NaCl, there was a significant reduction for most cultivars: Barcelona and Tonda Gentile Romana decreased to 2.74 and 2.28 (84.5% and 87.1% reductions), and Yamhill declined to 3.01 (an 82.7% decrease), while Tonda di Giffoni maintained the highest ratio at 8.49 (a 43.6% reduction).

Further reductions occurred at 50 mM NaCl: Barcelona and Tonda Gentile Romana dropped to 1.49 and 1.43, while Tonda di Giffoni and Yamhill maintained slightly higher ratios of 2.24 and 1.75. At 75 mM NaCl, the ratios reached their lowest values: Barcelona at 0.74, Tonda Gentile Romana at 0.83, Yamhill at 0.93, and Tonda di Giffoni maintaining the highest ratio at 1.20.

These K^+/Na^+ ratio patterns strongly correlated with biomass preservation under salt stress, showing high correlations with both fresh and dry weight (a Kendall correlation coefficient of 0.758 in both cases).

The organ-specific K^+/Na^+ ratios showed distinct patterns (Table S17 and Figure S14). The control leaves maintained the highest ratio (36.62), followed by the stems (18.06), wood (7.33), and roots (5.77). The 25 mM NaCl treatment reduced these ratios substantially: it decreased to 8.80 in the leaves (a 76% reduction), 1.54 in the roots (a 73.3% reduction), 4.99 in the stems (a 72.4% reduction), and 1.19 in the wood (an 83.8% reduction). At 75 mM NaCl, all organs showed their lowest ratios: leaves (1.94), roots (0.38), stems (1.05), and wood (0.32).

3.4.7. The Calcium/Sodium Ratio

The control conditions exhibited high Ca^{2+}/Na^+ ratios across all genotypes, indicating efficient calcium retention relative to sodium retention under normal growth conditions (Table S18 and Figure S15). Tonda Gentile Romana and Yamhill showed the highest ratios (27.51 and 27.28), while Barcelona and Tonda di Giffoni maintained slightly lower ratios (22.70 and 20.09). The 25 mM NaCl treatment induced substantial declines, with Tonda di Giffoni maintaining the highest ratio (11.71, a 41.7% reduction), followed by Yamhill (7.18, a 73.7% decrease). Barcelona and Tonda Gentile Romana showed the largest reductions, dropping to 6.05 and 5.95 (73.4% and 78.4% decreases).

At 50 mM NaCl, the ratios continued to decline significantly. Tonda di Giffoni maintained the highest ratio (5.28, a 54.9% reduction from 25 mM), while Yamhill and Barcelona dropped to 3.12 and 3.00 (56.5% and 50.4% reductions). Tonda Gentile Romana showed the lowest ratio (2.46, a 58.7% reduction). The 75 mM NaCl treatment resulted in the lowest Ca^{2+}/Na^+ ratios across all genotypes: Tonda di Giffoni maintained the highest ratio (3.37, a 71.2% reduction from the control), while Barcelona, Tonda Gentile Romana, and Yamhill showed similar low ratios (2.00, 2.02, and 1.97, representing reductions of 91.2%, 92.7%, and 92.8%).

The cultivar-specific Ca^{2+}/Na^+ ratios also exhibited strong correlations with the biomass responses, as evidenced by high correlations with the fresh and dry weights (Kendall correlation coefficients of 0.727 and 0.848, respectively).

The organ-specific analysis revealed distinct patterns in the Ca^{2+}/Na^+ ratios (Table S19 and Figure S16). Under the control conditions, the leaves maintained the highest ratio (28.97), with the roots, stems, and wood showing slightly lower values (26.04, 19.71, and 22.87). The 25 mM NaCl treatment significantly reduced these ratios: they dropped to 4.37 in the leaves (an 84.9% reduction), while they decreased to 9.19 and 10.71 in the roots and stems (64.7% and 45.6% reductions). They declined to 6.62 in the wood (a 71.1% reduction).

At 50 mM NaCl, the declining trend continued: it decreased to 2.13 in the leaves (a 51.3% reduction from 25 mM), it dropped to 5.31 and 3.48 in the roots and stems (42.3%

and 67.5% reductions), and it declined to 2.93 in the wood (a 55.8% reduction). The 75 mM NaCl treatment resulted in the lowest Ca^{2+}/Na^+ ratios across all organs: they dropped to 1.30 in the leaves (a 95.5% reduction from the control), while they declined to 4.35, 2.39, and 1.33 in the roots, stems, and wood (reductions of 83.3%, 87.9%, and 94.2% from the initial values).

4. Discussion

4.1. Growth Response to Salinity Stress

Fresh weight responses reflect the complex interaction between water relations and growth vigor under salt stress. Tonda di Giffoni's superior performance suggests genetic traits favoring efficient water uptake and retention mechanisms. The minimal difference between Tonda di Giffoni and Barcelona in the control conditions indicates their comparable baseline water use efficiency, aligning with previous observations on genotype-specific growth responses [2,9].

In contrast, the significantly lower fresh weights of Tonda Gentile Romana and Yamhill suggest their inherently limited capacity for biomass production. Tonda Gentile Romana, in particular, showed a severe decline across all salinity levels, suggesting that it is more susceptible to salt stress, potentially due to ineffective ion exclusion or poor osmotic regulation mechanisms [54]. This contrasts with Tonda di Giffoni's relatively higher fresh weights under 75 mM NaCl, which suggests that this genotype may have a robust mechanism of salinity tolerance, supporting findings that the genotypic variability in salt stress responses reflects differences in physiological and molecular adaptations [32].

The overall 81.9% reduction in the fresh weight from the control conditions to 75 mM NaCl reflects the profound impact of salinity stress on plant physiology. The most substantial reduction occurred between the control and 25 mM NaCl (59.2%) conditions, indicating that these plants exhibit acute sensitivity to the initial stages of salt exposure. The smaller declines at higher concentrations may reflect adaptative responses or physiological saturation points. These observations align with the established understanding of how salinity stress disrupts cellular water potential, leading to reduced biomass and growth [54,55].

The organ-specific responses to salinity stress revealed distinct patterns of resilience. The leaves showed the highest initial fresh weight, reflecting their primary photosynthetic role [31], but exhibited a sharp decline at 25 mM NaCl, with early defoliation by the fourth fortnight at higher concentrations (50 and 75 mM NaCl). This pattern corroborates the observations reported by Parihar et al. [56] that prolonged Na^+ and $Cl-$ transport to transpiring leaves eventually results in toxic accumulation and leaf death. The roots and wood demonstrated greater resilience, maintaining higher fresh weights even at 75 mM NaCl, supporting their critical roles in ion compartmentalization and structural stability [57]. The stems showed the most severe reductions, likely due to their exposure to ionic toxicity during salt transport [27].

The dry weight reductions paralleled the fresh weight patterns, with an 81.5% overall decline from the control conditions to 75 mM NaCl. The steep initial decline between the control and 25 mM NaCl (61.4%) highlights the immediate impact of salinity on growth, while the smaller subsequent reductions indicate physiological adaptation limits. These results parallel the work reported by Chartzoulakis [23] in olive trees, where the extent of the reduction varied with the exposure duration and cultivar characteristics.

4.2. Physiological Responses to Salinity Stress

4.2.1. Photosynthetic Performance, Electron Transport Chain Response, and Energy Dissipation

The performance index on an absorption basis (PI_abs) serves as a comprehensive indicator of photochemical efficiency under abiotic stress, as it integrates energy absorption, excitation trapping, and electron transport capabilities [58]. Analysis of the PI_abs values revealed significant genotypic variation in the plants' ability to maintain their photosynthetic function under salinity stress, highlighting differences in the stress tolerance mechanisms across the cultivars studied. Tonda di Giffoni stood out for its ability to maintain positive PI_abs values even under high salinity conditions, suggesting that this genotype possesses highly efficient photosynthetic machinery and robust energy capture mechanisms, while Yamhill's sharp decline to -61.62 at 75 mM NaCl indicated a severe compromise of PSII functionality and energy capture efficiency. This genotypic variation in the PSII response aligns with previous findings in other *C. avellana* cultivars ('Segorb', 'Ronde de Piemant', 'Fertile de Coutard', and 'Negret'), where Porghahreman et al. [32] demonstrated that salinity impacts PSII through both ionic and osmotic stress mechanisms, with the cultivars maintaining lower sodium and chloride accumulation and a high potassium content (e.g., 'Fertile de Coutard') showing the best photosynthetic performance (in terms of the smallest decrease in F_v/F_m) under salinity stress.

The disruption patterns in the electron transport chain provided additional insights into stress-induced photoinhibition. Tonda di Giffoni's maintenance of stable REo/RC values across the treatments indicates its robust energy transfer mechanisms and minimal electron transport chain disruption, characteristics identified by Strasser et al. [45] as hallmarks of stress tolerance. The persistent negative REo/RC values in Tonda Gentile Romana indicate chronic disruption of electron transport processes. Barcelona's fluctuating responses and Yamhill's extreme variations, particularly at 75 mM NaCl, demonstrate unstable adaptation mechanisms. These observations validate the work reported by Baker [59] and Murchie and Lawson [60] on chlorophyll fluorescence as a sensitive indicator of energy transfer disruptions under abiotic stress.

With regard to the energy dissipation patterns, analyzed through the Dio/RC values, distinct genotype variations were observed in their capacity to manage excess energy under salt stress. Tonda di Giffoni's lower Dio/RC values demonstrate superior photoprotective mechanisms, while Barcelona and Yamhill showed high dissipation rates, indicating less efficient energy management and significant photodamage. Tonda Gentile Romana displayed moderate dissipation rates, suggesting its intermediate stress adaptation capacity. These responses align with the findings by Lu [61] regarding the critical function of non-photochemical quenching in stress tolerance and are consistent with the work by Catoni et al. [62], who demonstrated that hazelnut saplings subjected to moderate and severe water stress enhanced their photoprotection mechanisms and excess energy dissipation capabilities, indicated by their modified carotenoid-to-chlorophyll ratios and altered PSII efficiency.

4.2.2. Temporal Adaptation Patterns

The temporal analysis revealed distinct phases in stress response development. The initial optimal performance in April (control conditions) contrasted with the emerging stress responses by June, particularly in sensitive genotypes like Yamhill and Barcelona. The September measurements demonstrated either successful long-term adaptation or cumulative damage, with Tonda di Giffoni showing a superior recovery and sustained functionality. This temporal pattern supports the findings by Jajoo [63] that prolonged

salinity exposure results in either successful adaptation or progressive photodamage, reflected in chlorophyll fluorescence patterns and photosynthetic efficiency changes.

4.3. Visual Symptoms and Plant Survival

4.3.1. Progressive Stress Response and Tissue Damage

The progression of visual symptoms in response to salinity stress reflects the complex mechanisms of salinity stress impacts. Following the observations of Shani and Ben-Gal [64], the reduced osmotic potential due to elevated salt levels significantly affected transpiration and photosynthesis, resulting in visible signs of stress such as leaf wilting and yellowing. These symptoms were particularly evident in Tonda Gentile Romana and Yamhill at 25 mM NaCl, indicating their heightened sensitivity to salt stress. In contrast, Barcelona and Tonda di Giffoni were able to maintain better tissue functionality, suggesting that these genotypes have evolved more effective mechanisms for dealing with salt-induced damage. This differential response aligns with the findings of Porghahreman et al. [32], who also observed that different hazelnut cultivars exhibit varying degrees of tolerance to salinity.

At the cellular level, salinity stress involves multiple mechanisms, disrupting cellular homeostasis and leading to the accumulation of toxic ions such as Na^+ and Cl^-. This disruption impairs cell function and triggers the production of reactive oxygen species (ROS), as described by Manishankar et al. [65]. The production of ROS further exacerbates oxidative stress, causing cellular damage. This was particularly evident in Yamhill and Tonda Gentile Romana, which exhibited higher levels of oxidative stress and more pronounced damage compared to the other genotypes. This suggests that these cultivars may lack robust mechanisms for mitigating ROS production or repairing oxidative damage, making them more vulnerable to the damaging effects of salinity.

4.3.2. Root System Adaptation Strategies

The root architecture analysis revealed important adaptive mechanisms for stress management. As described in the model proposed by Munns and Tester [54], extended root systems improved both toxic ion management and growth maintenance. Yamhill's extensive vertical root system exemplifies this advantage, with Tavakkoli et al. [66] confirming that such architecture enhances stress management and reduces tissue damage.

Conversely, Tonda Gentile Romana's compact root structure limited its stress avoidance capability, supporting the findings by Lupo et al. [67] regarding the importance of root exploration in salt stress management. The dense root architecture of Tonda di Giffoni enhanced its stress tolerance capacity, aligning with the emphasis by Zhang et al. [57] on the root density's role in mitigating salinity's effects.

4.3.3. Survival Strategy Differentiation

The survival patterns revealed distinct genotypic strategies for stress management. Yamhill's extended survival across all of the NaCl concentrations suggests effective stress management mechanisms. Tonda di Giffoni demonstrated intermediate tolerance through efficient stress management, supporting the findings by Zhang et al. [57] on the importance of cellular adaptation mechanisms.

These morphological responses and survival patterns were closely linked to underlying ionic homeostasis mechanisms, which will be discussed in detail in the following section.

4.4. Ionic Relations and Mineral Homeostasis

4.4.1. Calcium Dynamics

Genotype-specific variations in the calcium response revealed intricate regulatory mechanisms underlying stress adaptation. The diverse functions of calcium—from osmotic regulation to membrane stabilization, cell wall strengthening, and secondary messaging—

underpin its vital role in stress tolerance, as demonstrated by Gilliham et al. [68]. In this study, Tonda di Giffoni exhibited superior calcium maintenance, exceeding Barcelona's calcium levels by 15.9%. This suggests that Tonda di Giffoni may possess more efficient calcium transport and storage mechanisms, which are crucial for managing stress-induced ionic imbalances. The comparable calcium levels between Yamhill and Tonda Gentile Romana suggest shared physiological mechanisms in calcium homeostasis, pointing to potentially similar genetic pathways controlling calcium transport and storage in these cultivars. These results parallel the findings reported by Porghahreman et al. [32] in other hazelnut cultivars, which demonstrated a strong correlation between ion regulation capacity and stress tolerance.

The progressive decline observed in the calcium concentration under increasing salinity (a 40% reduction at 75 mM NaCl) supports the findings by Rengel [69] on sodium's interference with calcium dynamics through multiple mechanisms: reduced plasma membrane binding, altered calcium flux patterns, and depleted endomembrane stores.

The distribution of calcium across the plant organs revealed distinct gradients, with the roots maintaining the highest concentrations, reflecting their fundamental role in nutrient acquisition and ionic regulation, as demonstrated by Rengel [69]. This accumulation pattern is facilitated by specialized transport mechanisms in the vacuolar membranes, including Ca^{2+}-ATPases and Ca^{2+}/H^+ exchangers, which regulate calcium sequestration [70]. The lower calcium concentrations in the wood and stem tissues align with the observations by Manishankar et al. [65] regarding tissue-specific calcium allocation, which is influenced by both structural function and transpirational flow patterns.

4.4.2. Potassium Regulation

Tonda di Giffoni demonstrated superior potassium accumulation, exceeding Tonda Gentile Romana's potassium content by 15.7%, reflecting significant genotype-specific differences in potassium uptake and transport. This variation aligns with the findings of Shabala and Pottosin [71] on how genotype-specific characteristics, particularly the root architecture and ion transport mechanisms, influence the potassium uptake efficiency under stress conditions.

The importance of genotypic control over root-to-shoot transport efficiency for K^+, as identified by Storey et al. [72], helps to explain these differential responses to salinity stress. The similarity in the potassium levels between Yamhill and Barcelona suggests that these genotypes may share common mechanisms for potassium homeostasis. However, further investigation is needed to understand the molecular pathways governing potassium regulation in these cultivars.

The observed decline in potassium content with increasing salinity, particularly the 45.9% reduction at 75 mM NaCl compared to the control conditions, is consistent with the findings of Munns and Tester [54], who attributed such declines to the competitive interactions between sodium and potassium at the root uptake sites. Elevated sodium levels in saline environments interfere with potassium acquisition by the roots, creating a competitive environment for ion uptake. This competition may limit potassium availability to the plant, impairing essential processes like photosynthesis, osmotic regulation, and stress signaling.

The distribution of potassium across the plant organs revealed striking patterns, with the leaf concentrations exceeding the levels in the wood by 13.9-fold. This preferential accumulation in the leaves supports the findings by Kant et al. [73] regarding potassium's critical functions in maintaining photosynthetic efficiency and regulating stomatal movements through osmotic adjustments and guard cell turgor control. While the minimal potassium content in the wood tissue aligns with its primary structural function, the roots

showed intermediate concentrations, reflecting their dual role in uptake and transport. Shabala and Cuin [74] emphasize that maintaining favorable cytosolic K^+/Na^+ ratios is essential for salt tolerance, achieved through the coordinated action of transport proteins and ion channels. The competition between potassium and sodium at root uptake sites, coupled with continuous transport to photosynthetically active tissues, creates dynamic concentration gradients across organs. These patterns support the observations by Storey et al. [72] on potassium's vital role in maintaining ion balance under saline conditions. The higher potassium content in the stems compared to that in the roots reflects their role in nutrient transport, while the dramatic reduction in the potassium levels across all organs from the control conditions to 75 mM NaCl (up to a 1.85-fold decrease) supports the findings by Shabala and Pottosin [71] regarding potassium's essential role in stress responses, where it functions as a crucial signaling molecule regulating osmotic adjustment and ionic balance.

4.4.3. Chloride Accumulation Patterns

The observed genotypic variation in chloride management reflects distinct stress adaptation strategies. Tonda Gentile Romana's high chloride accumulation, exceeding Tonda di Giffoni's content by 30.3%, aligns with the findings by Tregeagle et al. [75] that salt tolerance correlates with a plant's ability to restrict chloride entry into the xylem and limit root-to-shoot transport. The higher chloride accumulation in Tonda Gentile Romana suggests that this cultivar may not be as efficient at excluding chloride from its vascular system, leading to more chloride being transported to the shoot tissues, where it can cause oxidative stress and ionic imbalance. On the other hand, Tonda di Giffoni's lower chloride accumulation suggests its more effective exclusion mechanisms and enhanced capacity for ion compartmentalization. This trait likely contributes to its superior resilience to salt stress, as it can prevent chloride from reaching sensitive metabolic tissues.

The dramatic increase in the chloride concentrations under salinity stress (481% higher at 75 mM NaCl compared to control) corresponds with the observations by Isayenkov and Maathuis [55] regarding the significant contribution of apoplastic transport to chloride uptake, particularly under high transpirational demand.

The organ-specific chloride distribution patterns revealed that the chloride concentrations in the leaves exceeded those in the wood by a 6.9-fold difference, reflecting strategic compartmentalization to protect metabolically active tissues from chloride toxicity. This finding supports the emphasis by Mansour [70] on the importance of vacuolar chloride compartmentalization in the leaves as a key mechanism of stress management. By sequestering chloride into the vacuoles, the plant reduces the potential for chloride to interfere with the cellular processes in the cytoplasm, such as photosynthesis and respiration. The wood tissue maintained the lowest chloride levels, while the roots showed intermediate concentrations between those in the wood and stems. This finding highlights the roots' dual role in both ion uptake and ion sequestration, protecting the shoot tissues from excessive chloride buildup. This pattern aligns with the findings by Rahneshan et al. [76] in pistachio rootstocks, where the roots are essential for regulating ion uptake and translocation to maintain ion balance and prevent toxic ion accumulation.

The differential chloride regulation patterns observed across all genotypes align with observations by Martin et al. [27] in woody perennials, where effective ion compartmentalization serves as a critical mechanism for salt tolerance. This genetic component of chloride management supports the findings by Negrão et al. [77] that salt tolerance mechanisms involve complex multigenic interactions determining a plant's capacity to manage ionic stress.

4.4.4. Sodium Homeostasis

The sodium accumulation patterns also revealed clear genotypic differences in their stress responses. Tonda Gentile Romana's higher sodium content (48.1% above that of Tonda di Giffoni) suggests its less effective sodium exclusion or vacuolar sequestration mechanisms, while Barcelona and Yamhill showed similar sodium accumulation patterns, potentially indicating shared physiological mechanisms governing the sodium dynamics. As discussed by Munns and Tester [54], the genetic factors influencing sodium transport significantly affect salinity tolerance, with better control over sodium influx correlating with enhanced stress resistance. The emphasis of Zhang et al. [57] on reducing Na^+ uptake as the most efficient approach to controlling accumulation and improving salt resistance provides context for these genotypic differences.

The organ-specific sodium distributions revealed highly heterogeneous patterns, with the leaves exhibiting concentrations 2.73-fold higher than those in the wood. This differential accumulation represents an adaptive mechanism whereby plants translocate excess sodium from the roots and stems to the aerial tissues for vacuolar sequestration, serving dual functions: protecting critical root functions and utilizing sodium as an osmolyte for maintaining water relations. This aligns with the findings by Mansour [70] on the crucial role of vacuolar Na^+ sequestration in minimizing cytosolic toxicity while enabling osmotic adjustment. This pattern supports the emphasis by Parida and Das [78] on ion compartmentalization and selective transport as essential strategies for maintaining ion homeostasis under salinity stress.

The low sodium content in the wood tissue reflects its minimal involvement in ion transport, consistent with its structural role [57]. The roots and stems exhibited intermediate sodium levels, reflecting their distinct roles in uptake and transport. Roots function as the primary entry point for sodium, showing a higher content than that in the stems due to their role as the first barrier against excessive influx. As noted by Trapp et al. [79], salt uptake depends on enzyme-mediated transport processes that can be overwhelmed under high salinity, leading to uncontrolled accumulation. The stems primarily serve as conduits for sodium transport, explaining their moderate accumulation patterns.

4.4.5. Potassium/Sodium Balance

The K^+/Na^+ ratio emerged as a key metric for the salt tolerance mechanisms in the hazelnut cultivars. Tonda di Giffoni's maintenance of higher K^+/Na^+ ratios (21.4% above Tonda Gentile Romana) demonstrates its superior ion transport regulation, particularly in favoring potassium retention while limiting sodium accumulation. This capacity for ion discrimination supports the emphasis by Munns and Tester [54] on genetic determinants of ion selectivity under salinity stress. The similarity between Yamhill and Barcelona's responses suggests shared genetic traits influencing their ion balance mechanisms.

The sharp decline in the K^+/Na^+ ratio with increasing salinity, particularly the 75.6% reduction at 25 mM NaCl relative to the control conditions, illustrates the significant disruption of potassium acquisition concurrent with enhanced sodium accumulation. These patterns mirror the results reported by Shabala and Pottosin [71] regarding ionic antagonism under salt stress. This pattern supports the identification by Negrão et al. [77] of three main salinity tolerance mechanisms: ion exclusion, tissue tolerance, and shoot ion-independent tolerance. The superior maintenance of the K^+/Na^+ ratios by certain genotypes, particularly Tonda di Giffoni, aligns with the findings by Luo et al. [33] in salt-tolerant Ping'ou hybrid hazelnuts. These genotypes likely employ robust ion transport regulation mechanisms, including enhanced activity of the K^+/Na^+ antiporters and selective ion channels, to preserve potassium homeostasis while mitigating sodium toxicity.

The organ-specific distribution of the K^+/Na^+ ratios, particularly the higher values in the leaves, underscores the prioritization of potassium in photosynthetically active tissues. Stems, wood, and roots showed significantly lower ratios, consistent with their structural roles and reduced metabolic demand for potassium. This distribution confirms the findings reported by Storey et al. [72] regarding preferential potassium allocation to metabolically active tissues, reflecting both physiological priorities and functional requirements under stress conditions.

4.4.6. Calcium/Sodium Interactions

The Ca^{2+}/Na^+ ratio analysis revealed complex patterns of ionic interactions under stress. Tonda di Giffoni's maintenance of higher Ca^{2+}/Na^+ ratios (19.8% above those in Barcelona) suggests its more effective mechanisms of sodium exclusion or calcium retention. This capability corresponds with the findings reported by Munns and Tester [54] regarding genotypic differences in ion transport and compartmentalization as determinants of salinity tolerance. The minimal differences between Yahmill and Tonda Gentile Romana further reinforce the hypothesis of similar ion regulation mechanisms resulting from shared genetic traits.

The dramatic reduction in the Ca^{2+}/Na^+ ratios under salinity stress (a 90.4% overall reduction) reflects the severity of the ionic imbalance. The sharp initial decline from the control conditions to 25 mM NaCl (68.4%) supports the description by Acosta-Motos et al. [31] of salt stress's progression, from initial osmotic effects to subsequent ionic toxicity. This response matches the results reported by Manishankar et al. [65] that elevated sodium concentrations can displace calcium from both pectin-associated cross-linking sites and plasma membrane binding sites, compromising cellular structural integrity and function. As emphasized by Gilliham et al. [68], calcium nutritional flow must be carefully regulated to prevent interference with signaling events, highlighting the complex balance required to maintain ion homeostasis under salinity stress.

Across the plant organs, the responses revealed that the roots maintained higher Ca^{2+}/Na^+ ratios (24.8% above those in wood), reflecting their critical role in ion uptake regulation and calcium accumulation. The leaves and stems showed intermediate ratios, in line with their roles in calcium transport and storage. This distribution pattern validates the research reported by Mansour [70] indicating that sodium and chloride must be either excluded or sequestered in the vacuoles to maintain adequate potassium and calcium levels for metabolic functions under saline conditions.

These findings demonstrate that salt tolerance in hazelnuts involves multiple integrated mechanisms: ion exclusion, compartmentation, and root architectural adaptations. The superior performance of Yamhill and Tonda di Giffoni under high salinity (75 mM NaCl) reflects their effective combination of these adaptation strategies.

4.5. Comparative Cultivar Performance

The analysis of the four hazelnut cultivars revealed distinct patterns of salt tolerance and stress adaptation mechanisms. To provide a comprehensive visual summary of the cultivars' performance across key physiological parameters, Table 1 presents a heatmap integrating multiple stress response indicators. This visualization captures the relative performance of each cultivar across different metrics, including photosynthetic efficiency, ion homeostasis, biomass retention, and survival capacity.

Tonda di Giffoni emerged as the superior performer, demonstrating sustained photosynthetic efficiency across the salinity treatments and excellent ion balance, as reflected in its consistently higher K^+/Na^+ ratios (8.49 at 25 mM NaCl) and Ca^{2+}/Na^+ ratios. Its ability to effectively limit Na^+ and Cl^- accumulation, combined with its superior biomass reten-

tion under stress, establishes it as the most suitable option for cultivation in moderately saline conditions.

Table 1. Hazelnut cultivar salt tolerance heatmap. The color gradient ranges from green (+3 on the numerical scale), indicating higher tolerance, to red (−3), representing lower tolerance.

Parameters/Cultivars	Tonda di Giffoni	Barcelona	Yamhill	Tonda Gentile Romana
Survival rate	3	1	2	−1
Photosynthetic efficiency (PI_abs)	3	1	−1	0
K^+/Na^+ ratio	3	1	2	−1
Ca^{2+}/Na^+ ratio	3	0	0	−1
Fresh weight retention	2	1	1	−2
Root system	2	1	2	−2
Chloride accumulation resistance	3	0	−1	−2

Barcelona exhibited a strong performance under low salinity (25 mM NaCl), with a moderate ion regulation capacity. However, its sharp decline in photosynthetic efficiency at higher salinity levels, despite maintaining a relatively good root architecture, suggests that its suitability is limited to areas with mild salinity.

Yamhill demonstrated a remarkable survival capacity despite its poor photosynthetic performance. It was characterized by extensive vertical root development and efficient Na^+ compartmentalization. These traits, along with moderate ion balance maintenance, identify it as a valuable genetic resource for breeding programs focused on stress resistance.

Tonda Gentile Romana consistently showed the highest sensitivity to salinity stress, accumulating the highest levels of Na^+ and Cl^-, maintaining the poorest ion balance ratios, and exhibiting limited root development. These characteristics indicate its unsuitability for cultivation in salt-affected areas.

4.6. Agricultural and Breeding Implications

This study's findings have significant implications for hazelnut cultivation in regions facing increasing soil salinity challenges. The genotypic variations in the salt tolerance mechanisms identified provide valuable insights for breeding programs and agricultural management strategies. Tonda di Giffoni's superior performance under moderate salinity conditions (25–50 mM NaCl) suggests its suitability for areas facing emerging salinity challenges, particularly in Mediterranean regions, where irrigation with brackish water is becoming more common.

This comprehensive physiological and biochemical characterization of the salt stress responses enables more accurate predictions of genotype performance under varying salinity conditions. Chlorophyll fluorescence parameters, particularly PI_abs and electron transport rates, have been identified as reliable early indicators of salt stress damage, allowing for timely management interventions, which may be used along with the leaf water potential and stomatal conductance measurements suggested by Cincera et al. [17] and Altieri et al. [18].

The established salinity thresholds for each genotype provide practical guidelines for irrigation management, though these greenhouse findings should be interpreted cautiously when extrapolating them to field conditions. Based on the survival analysis, all of the cultivars demonstrated tolerance to irrigation water up to 3 dS m^{-1} (≈25 mM NaCl) under controlled conditions. When using water above 3 dS m^{-1}, the cultivar selection appears to be critical—Tonda di Giffoni and Yamhill maintained viability, while Barcelona and Tonda Gentile Romana showed reduced survival. While our results suggest the irrigation water's electrical conductivity should not exceed 6 dS m^{-1} (approximately 50 mM NaCl) even for

tolerant cultivars like Tonda di Giffoni, field validation is essential. Moreover, this threshold represents survival conditions rather than the optimal production parameters—under field conditions, using irrigation water with such high salinity would severely compromise yield and growth potential, making it economically unfeasible for commercial production. In our greenhouse study, the salt balance was maintained through a 20–30% leaching fraction—a condition that may be impractical in commercial orchards due to water availability constraints and economic considerations. For practical orchard management focusing on optimal yield and growth, the irrigation water's electrical conductivity should not exceed 3.0 dS m^{-1}, as higher values would significantly impact production, even if plant survival is possible.

The irrigation duration should be adjusted based on EC measurements to maintain the optimal salt balance in the root zone. The irrigation frequency should be adapted according to cultivar tolerance. Sensitive cultivars like Tonda Gentile Romana benefit from more frequent, lighter irrigations to avoid salt accumulation, while tolerant cultivars like Tonda di Giffoni can maintain productivity under standard irrigation scheduling. Effective soil salinity management requires regular EC monitoring at multiple depths throughout the root zone. This can be complemented by applying organic mulches to reduce evaporation and salt accumulation at the soil surface. Installation of adequate drainage systems is essential for long-term salinity management, particularly in areas with poor natural drainage.

The differential ion accumulation patterns observed among genotypes provide actionable insights for fertilization strategies under saline conditions. Specifically, potassium and calcium supplementation can be optimized to maintain the optimal ion ratios, enhancing plant resilience and productivity.

These findings can contribute to the development of targeted approaches for enhancing hazelnut production under saline conditions. This includes genotype selection based on location-specific salinity levels, the optimization of irrigation practices, and the development of appropriate nutrient management strategies.

4.7. Study Limitations and Future Research Directions

This study identifies several areas that require further investigation from a research perspective. Our findings, though they provide valuable insights into salt tolerance mechanisms, are constrained by several experimental limitations. While detailed physiological and ionic responses were captured, data gaps remain regarding the nut yield and quality impacts under saline conditions. The five-month experimental period proved sufficient for observing the acute stress responses yet precluded an evaluation of long-term adaptation mechanisms.

The controlled greenhouse environment, though it enabled precise manipulation of the stress conditions, presents significant limitations. First, it does not fully represent the complexity in the field, where multiple environmental factors interact with salinity stress. Second, the root system development and architecture analysis were limited by the pot conditions. Third, and importantly, this approach cannot capture the natural history of salt stress responses—how hazelnut cultivars might develop adaptive mechanisms over multiple seasons when they are exposed to gradually increasing salinity under field conditions.

The irrigation management strategy—maintaining the soil moisture at field capacity with a 20–30% leaching fraction—differs from typical orchard conditions. While the emphasis on NaCl-induced stress is undoubtedly valuable from an experimental standpoint, it does not encompass the broader spectrum of salt compositions commonly encountered in agricultural settings, nor does it account for their interactions with other environmental stressors.

To address these limitations and confirm the greenhouse findings, several research directions are recommended. Field validation trials are necessary under various environmental conditions, examining different water salinity levels, SAR irrigation values, deficit irrigation approaches, and soil types. Long-term observational studies across multiple growing seasons are essential to assess the genotype performance over time, particularly in mature trees, where the nut production can be properly evaluated and natural adaptation processes can be documented. Further exploration of the molecular mechanisms underlying salt tolerance patterns, particularly in Tonda di Giffoni, could enhance the efficiency of breeding programs through gene identification and marker development. Recent findings on the *DREB* and *AP2* genes in hazelnut salt stress response [32] provide promising starting points for such molecular investigations.

Future research should expand into detailed physiological studies examining osmolyte accumulation and antioxidant responses. Additionally, economic feasibility assessments and the development of efficient screening protocols for salt tolerance evaluation in hazelnut cultivars are recommended.

5. Conclusions

The comparative analysis of the salt tolerance mechanisms in four hazelnut cultivars revealed distinct physiological and morphological adaptations to salinity stress. Tonda di Giffoni emerged as the most salt-tolerant cultivar, maintaining superior photosynthetic efficiency and ion homeostasis under moderate salinity levels. This cultivar's enhanced performance was characterized by efficient Na^+ exclusion, maintained K^+/Na^+ and Ca^{2+}/Na^+ ratios, and effective operation of the photosynthetic machinery even at elevated salt concentrations. In contrast, Tonda Gentile Romana exhibited high sensitivity to salinity, while Barcelona and Yamhill showed intermediate responses, with varying adaptation mechanisms.

Our findings establish 50 mM NaCl as a critical physiological threshold beyond which all cultivars exhibited significant stress symptoms and reduced growth. This threshold has important implications for irrigation management in regions where salinity poses a growing challenge to hazelnut cultivation. This study demonstrates that salt tolerance in hazelnuts results from the coordinated action of multiple mechanisms, including ion exclusion at the root level, efficient vacuolar compartmentalization, and maintenance of photosynthetic capacity. The root system architecture emerged as a crucial factor in stress adaptation, with more extensive root systems correlating with enhanced salt tolerance.

These insights provide practical tools for sustainable hazelnut cultivation in salt-affected regions. The physiological thresholds identified can guide irrigation management with saline water, while the cultivar-specific tolerance profiles enable informed decisions about the genotype selection based on local salinity conditions. For regions facing moderate salinity challenges (25–50 mM NaCl), Tonda di Giffoni offers a viable option for maintaining productive orchards. In areas with a higher salinity risk, our findings suggest the need for appropriate management strategies, including enhanced drainage systems and careful irrigation scheduling, particularly when using brackish water.

The comprehensive characterization of the cultivar responses could also contribute to climate change adaptation strategies in hazelnut production. As soil salinization and water quality issues intensify globally, the stress tolerance mechanisms identified here can inform breeding programs targeting enhanced resilience. The multi-parameter approach used in this study—combining survival assessment, physiological monitoring, and ion relations—provides a robust framework for screening salt-tolerant genotypes, supporting the development of better-adapted cultivars for sustainable hazelnut production in marginal areas.

Supplementary Materials: The following supporting information can be downloaded at https://www.mdpi.com/article/10.3390/agronomy15010148/s1. Figure S1: Robust confidence intervals and robust homogeneous groups for fresh weight as a function of the genotype × treatment interaction; Figure S2: Robust confidence intervals and robust homogeneous groups for fresh weight as a function of the treatment × organ interaction; Figure S3: Robust confidence intervals and robust homogeneous groups for dry weight as a function of the genotype × treatment interaction; Figure S4: Robust confidence intervals and robust homogeneous groups for dry weight as a function of the organ × treatment interaction; Figure S5: Robust confidence intervals and robust homogeneous groups for Ca^{2+} as a function of the genotype × treatment interaction; Figure S6: Robust confidence intervals and robust homogeneous groups for Ca^{2+} as a function of the treatment × organ interaction; Figure S7: Robust confidence intervals and robust homogeneous groups for K^+ as a function of the genotype × treatment interaction; Figure S8: Robust confidence intervals and robust homogeneous groups for K^+ as a function of the treatment × organ interaction; Figure S9: Robust confidence intervals and robust homogeneous groups for Cl^- as a function of the genotype × treatment interaction; Figure S10: Robust confidence intervals and robust homogeneous groups for Cl^- as a function of the treatment × organ interaction; Figure S11: Robust confidence intervals and robust homogeneous groups for Na^+ as a function of the genotype × treatment interaction; Figure S12: Robust confidence intervals and robust homogeneous groups for Na^+ as a function of the treatment × organ interaction; Figure S13: Robust confidence intervals and robust homogeneous groups for K^+/Na^+ as a function of the genotype × treatment interaction; Figure S14: Robust confidence intervals and robust homogeneous groups for K^+/Na^+ as a function of the treatment × organ interaction; Figure S15: Robust confidence intervals and robust homogeneous groups for Ca^{2+}/Na^+ as a function of the genotype by treatment interaction; Figure S16: Robust confidence intervals and robust homogeneous groups for Ca^{2+}/Na^+ as a function of the treatment × organ interaction; Table S1: Statistical data for fresh weight as a function of the rootstock genotype × treatment interaction; Table S2: Statistical data for fresh weight as a function of the treatment × organ interaction; Table S3: Statistical data for dry weight as a function of the rootstock genotype × treatment interaction; Table S4: Statistical data for dry weight as a function of the treatment × organ interaction; Table S5: Descriptive statistics of fluorimeter measurements; Table S6: Descriptive statistics and robustness analysis of ion concentrations, biomass parameters, and ion ratios in plant tissue samples; Table S7: Robust comparisons of the group *p*-values for each of the factors along with their interactions; Table S8: Statistical data for Ca^{2+} content as a function of the rootstock genotype × treatment interaction; Table S9: Statistical data for Ca^{2+} content as a function of the treatment × organ interaction; Table S10: Statistical data for K^+ content as a function of the rootstock genotype × treatment interaction; Table S11: Statistical data for K^+ content as a function of the treatment × organ interaction; Table S12: Statistical data for Cl^- content as a function of the rootstock genotype × treatment interaction; Table S13: Statistical data for Cl^- content as a function of the treatment × organ interaction; Table S14: Statistical data for Na^+ content as a function of the rootstock genotype × treatment interaction; Table S15: Statistical data for Na^+ content as a function of the treatment × organ interaction; Table S16: Statistical data for K^+/Na^+ ratio as a function of the rootstock genotype × treatment interaction; Table S17: Statistical data for K^+/Na^+ ratio as a function of the treatment × organ interaction; Table S18: Statistical data for Ca^{2+}/Na^+ ratio as a function of the rootstock genotype × treatment interaction; Table S19: Statistical data for Ca^{2+}/Na^+ ratio as a function of the treatment × organ interaction.

Author Contributions: Conceptualization: X.R.-G., J.C.-G. and P.M.-R. Methodology: M.V.-M., J.C.-G., L.A.-R. and P.M.-R. Software: L.A.-R. Validation: J.C.-G. Formal analysis: X.R.-G., M.V.-M., J.C.-G., L.A.-R. and P.M.-R. Investigation: X.R.-G., M.V.-M., J.C.-G. and P.M.-R. Resources: X.R.-G. Data curation: L.A.-R. Writing—original draft preparation: X.R.-G., M.V.-M., J.C.-G., L.A.-R. and P.M.-R. Writing—review and editing: X.R.-G. and P.M.-R. Visualization: X.R.-G., J.C.-G. and L.A.-R. Supervision: M.V.-M. and J.C.-G. All authors have read and agreed to the published version of the manuscript.

Data Availability Statement: All of the data supporting the findings of this study are available within the paper and its Supplementary Information. Should any raw data files be needed in another format, they are available from the corresponding author upon reasonable request.

Conflicts of Interest: Author Xavier Rius-Garcia was employed by the company Agromillora Group. All authors declare that the research was conducted in the absence of any commercial or financial relationships that could be construed as a potential conflict of interest.

Abbreviations

The following abbreviations are used in this manuscript:

Area	Area above the fluorescence induction curve between F_0 and F_m. Related to the pool size of the electron acceptors in the photosynthetic electron transport chain.
CAGR	Compound annual growth rate.
DIo/CSo	Energy dissipated in the form of heat and fluorescence per cross-section.
DIo/RC	Energy dissipated in the form of heat and fluorescence per reaction center.
EC	Electrical conductivity.
ETo/RC	Electron transport rate per reaction center.
F_0	Initial fluorescence.
F_m	Maximum fluorescence.
F_v	Variable fluorescence.
F_v/F_m	Maximum PSII quantum efficiency when all reaction centers are open.
N	QA turnover number, i.e., the number of times QA is reduced and oxidized during the measurement.
OJIP	Chlorophyll fluorescence transient phases O, J, I, and P.
PI_abs	Performance index on an absorption basis.
PSII	Photosystem II.
pXRF	Portable X-ray fluorescence.
QA	Primary quinone electron acceptor.
REo/RC	Electron transport rate per reaction center, i.e., the rate of electron transport beyond QA per reaction center.
ROS	Reactive oxygen species.
SAR	Sodium adsorption ratio.
Sm	Normalized total complementary area above the OJIP transient. Related to the energy needed to close all PSII reaction centers.
Vj	Relative variable fluorescence at the J-step of the OJIP fluorescence transient. Provides information about the reduction state of the primary quinone electron acceptor.
$\varphi(Po)$	Maximum quantum yield of primary photochemistry.
$\psi(Eo)$	Efficiency with which a trapped exciton can move an electron into the electron transport chain beyond QA.

References

1. Silvestri, C.; Bacchetta, L.; Bellincontro, A.; Cristofori, V. Advances in cultivar choice, hazelnut orchard management, and nut storage to enhance product quality and safety: An overview. *J. Sci. Food Agric.* **2021**, *101*, 27–43. [CrossRef] [PubMed]
2. Solar, A.; Stampar, F. Characterisation of selected hazelnut cultivars: Phenology, growing and yielding capacity, market quality and nutraceutical value. *J. Sci. Food Agric.* **2011**, *91*, 1205–1212. [CrossRef] [PubMed]
3. An, N.; Turp, M.T.; Türkeş, M.; Kurnaz, M.L. Mid-term impact of climate change on hazelnut yield. *Agriculture* **2020**, *10*, 159. [CrossRef]
4. Vinci, A.; Di Lena, B.; Portarena, S.; Farinelli, D. Trend analysis of different climate parameters and watering requirements for hazelnut in Central Italy related to climate change. *Horticulturae* **2023**, *9*, 593. [CrossRef]
5. Moine, A.; Chitarra, W.; Nerva, L.; Agliassa, C.; Gambino, G.; Secchi, F.; Pagliarani, C.; Boccacci, P. Grafting with non-suckering rootstock increases drought tolerance in *Corylus avellana* L. through physiological and biochemical adjustments. *Physiol. Plant.* **2024**, *176*, e70003. [CrossRef]
6. Blagoeva, E.; Nikolova, M. Growth dynamics of hazelnut (*Corylus* spp.) grafted by different techniques. *Bull. Univ. Agric. Sci. Vet. Med. Cluj-Napoca Hortic.* **2010**, *67*, 96–100. [CrossRef]

7. Rovira, M.; Hermoso, J.F.; Romero, A.J. Performance of hazelnut cultivars from Oregon, Italy, and Spain, in Northeastern Spain. *HortTechnology* **2017**, *27*, 631–638. [CrossRef]

8. Tous, J.; Romero, A.; Plana, J. El cultivo del avellano en España. *Frutic. Prof.* **2009**, *185*, 5–13.

9. Grau, P.; Bastias, R. Productivity and yield efficiency of hazelnut (*Corylus avellana* L.) cultivars in Chile. *Acta Hortic.* **2005**, *686*, 57–64. [CrossRef]

10. Salimi, S.; Hoseinova, S. Selecting hazelnut (*Corylus avellana* L.) rootstocks for different climatic conditions of Iran. *Crop Breed. J.* **2012**, *2*, 139–144. [CrossRef]

11. Mehlenbacher, S.A.; Smith, D.C.; McCluskey, R.L. 'Yamhill' hazelnut. *HortScience* **2009**, *44*, 845–847. [CrossRef]

12. Hazelnut Hub. Understanding the Unique Traits of the Barcelona Hazelnut. Available online: https://hazelnuthub.com/understanding-the-unique-traits-of-the-barcelona-hazelnut/ (accessed on 16 December 2024).

13. Ortega-Farías, S.; Villalobos-Soublett, E.; Riveros-Burgos, C.; Zúñiga, M.; Ahumada-Orellana, L.E. Effect of irrigation cut-off strategies on yield, water productivity and gas exchange in a drip-irrigated hazelnut (*Corylus avellana* L. cv. Tonda di Giffoni) orchard under semiarid conditions. *Agric. Water Manag.* **2020**, *238*, 106173. [CrossRef]

14. Bignami, C.; Cristofori, V.; Ghini, P.; Rugini, E. Effects of irrigation on growth and yield components of hazelnut (*Corylus avellana* L.) in Central Italy. *Acta Hortic.* **2009**, *845*, 309–314. [CrossRef]

15. Marsal, J.; Girona, J.; Mata, M. Leaf water relation parameters in almond compared to hazelnut trees during a deficit irrigation period. *J. Am. Soc. Hortic. Sci.* **1997**, *122*, 582–587. [CrossRef]

16. Pasqualotto, G.; Carraro, V.; Conati, S.; Chloé, C.; Salaün, G.; Mercadal, M.; Vacca, A.; Castagna, A.; Utili, G.; Lisperguer, M.J.; et al. Stomatal sensitivity in *Corylus avellana* (L.): First analysis from a global dataset. *Acta Hortic.* **2018**, *1226*, 181–188. [CrossRef]

17. Cincera, I.; Frioni, T.; Ughini, V.; Poni, S.; Farinelli, D.; Tombesi, S. Intra-specific variability of stomatal sensitivity to vapour pressure deficit in *Corylus avellana* L.: A candidate factor influencing different adaptability to different climates? *J. Plant Physiol.* **2019**, *232*, 241–247. [CrossRef] [PubMed]

18. Altieri, G.; Wiman, N.G.; Santoro, F.; Amato, M.; Celano, G. Assessment of leaf water potential and stomatal conductance as early signs of stress in young hazelnut tree in Willamette valley. *Sci. Hortic.* **2024**, *327*, 112817. [CrossRef]

19. Baldwin, B. The Effects of Site and Seasonal Conditions on Nut Yield and Kernel Quality of Hazelnut Genotypes Grown in Australia. *Acta Hortic.* **2009**, *845*, 83–88. [CrossRef]

20. Kramer, I.; Mau, Y. Review: Modeling the Effects of Salinity and Sodicity in Agricultural Systems. *Water Resour. Res.* **2023**, *59*, e2023WR034750. [CrossRef]

21. Liu, X. Increasing competition for water resources in the food and energy industries. *PLoS ONE* **2024**, *19*, e0312836. [CrossRef]

22. Pereira, L.S. Water, agriculture and food: Challenges and issues. *Water Resour. Manag.* **2017**, *31*, 2985–2999. [CrossRef]

23. Chartzoulakis, K.S. Salinity and olive: Growth, salt tolerance, photosynthesis and yield. *Agric. Water Manag.* **2005**, *78*, 108–121. [CrossRef]

24. Measho, S.; Li, F.; Pellikka, P.; Tian, C.; Hirwa, H.; Xu, N.; Qiao, Y.; Khasanov, S.; Kulmatov, R.; Chen, G. Soil salinity variations and associated implications for agriculture and land resources development using remote sensing datasets in Central Asia. *Remote Sens.* **2022**, *14*, 2501. [CrossRef]

25. Butcher, K.; Wick, A.F.; DeSutter, T.; Chatterjee, A.; Harmon, J. Soil salinity: A threat to global food security. *Agron. J.* **2016**, *108*, 2189–2200. [CrossRef]

26. Hassani, A.; Azapagic, A.; Shokri, N. Predicting long-term dynamics of soil salinity and sodicity on a global scale. *Proc. Natl. Acad. Sci. USA* **2020**, *117*, 33017–33027. [CrossRef]

27. Martin, L.; Vila, H.; Bottini, R.; Berli, F. Rootstocks increase grapevine tolerance to NaCl through ion compartmentalization and exclusion. *Acta Physiol. Plant.* **2020**, *42*, 145. [CrossRef]

28. Hasegawa, P.M.; Bressan, R.A.; Zhu, J.-K.; Bohnert, H.J. Plant cellular and molecular responses to high salinity. *Annu. Rev. Plant Physiol. Plant Mol. Biol.* **2000**, *51*, 463–499. [CrossRef]

29. Khan, M.M.; Akram, M.T.; Qadri, R.W.K.; Al-Yahyai, R. Role of grapevine rootstocks in mitigating environmental stresses: A review. *J. Agric. Mar. Sci.* **2020**, *25*, 1–12. [CrossRef]

30. Ashraf, M.; Harris, P.J.C. Photosynthesis under stressful environments: An overview. *Photosynthetica* **2013**, *51*, 163–190. [CrossRef]

31. Acosta-Motos, J.; Ortuño, M.; Bernal-Vicente, A.; Diaz-Vivancos, P.; Sanchez-Blanco, M.; Hernandez, J. Plant responses to salt stress: Adaptive mechanisms. *Agronomy* **2017**, *7*, 18. [CrossRef]

32. Porghahreman, F.; Fatahi, R.; Zamani, Z.; Sallom, A. Morphological, physiological and molecular responses of four hazelnut (*Corylus avellana*) cultivars under NaCl salinity stress. *J. Plant Growth Regul.* **2024**, *43*, 3878–3895. [CrossRef]

33. Luo, D.; Song, F.; Lu, M.; Shi, Y.; Ma, Q. Salt-stress-induced ion transport contributes to K^+/Na^+ homeostasis in roots of Ping'ou hybrid hazelnut. *Forests* **2023**, *14*, 1651. [CrossRef]

34. Hoagland, D.R.; Arnon, D.I. *The Water-Culture Method for Growing Plants Without Soil*; College of Agriculture–University of California; California Agricultural Experiment Station: Berkeley, CA, USA, 1950; p. 31.

35. Perica, S.; Goreta, S.; Selak, G.V. Growth, biomass allocation and leaf ion concentration of seven olive (*Olea europaea* L.) cultivars under increased salinity. *Sci. Hortic.* **2008**, *117*, 123–129. [CrossRef]

36. Sapkota, Y.; McDonald, L.M.; Griggs, T.C.; Basden, T.J.; Drake, B.L. Portable X-ray fluorescence spectroscopy for rapid and cost-effective determination of elemental composition of ground forage. *Front. Plant Sci.* **2019**, *10*, 317. [CrossRef] [PubMed]

37. Towett, E.K.; Shepherd, K.D.; Lee Drake, B. Plant elemental composition and portable X-ray fluorescence (pXRF) spectroscopy: Quantification under different analytical parameters. *X-Ray Spectrom.* **2016**, *45*, 117–124. [CrossRef]

38. Antonangelo, J.; Zhang, H. Soil and plant nutrient analysis with a portable XRF probe using a single calibration. *Agronomy* **2021**, *11*, 2118. [CrossRef]

39. McGladdery, C.; Weindorf, D.C.; Chakraborty, S.; Li, B.; Paulette, L.; Podar, D.; Pearson, D.; Kusi, N.Y.O.; Duda, B. Elemental assessment of vegetation via portable X-ray fluorescence (pXRF) spectrometry. *J. Environ. Manag.* **2018**, *210*, 210–225. [CrossRef]

40. Singh, V.K.; Sharma, N.; Singh, V.K. Application of X-ray fluorescence spectrometry in plant science: Solutions, threats, and opportunities. *X-Ray Spectrom.* **2021**, *51*, 304–327. [CrossRef]

41. Jones, J.B.; Case, V.W. Sampling, handling, and analyzing plant tissue samples. In *Soil Testing and Plant Analysis*, 3rd ed.; Westerman, R.L., Ed.; Soil Science Society of America: Madison, WI, USA, 2018; Volume 3, pp. 389–427.

42. Kalra, Y. *Handbook of Reference Methods for Plant Analysis*; CRC Press: Boca Raton, FL, USA, 1997; p. 320. [CrossRef]

43. Kalaji, H.M.; Schansker, G.; Ladle, R.J.; Goltsev, V.; Bosa, K.; Allakhverdiev, S.I.; Brestic, M.; Bussotti, F.; Calatayud, A.; Dąbrowski, P.; et al. Frequently asked questions about in vivo chlorophyll fluorescence: Practical issues. *Photosynth. Res.* **2014**, *122*, 121–158. [CrossRef] [PubMed]

44. Stirbet, A.; Govindjee. On the relation between the Kautsky effect (chlorophyll a fluorescence induction) and Photosystem II: Basics and applications of the OJIP fluorescence transient. *J. Photochem. Photobiol. B Biol.* **2011**, *104*, 236–257. [CrossRef] [PubMed]

45. Strasser, R.J.; Tsimilli-Michael, M.; Srivastava, A. Analysis of the chlorophyll a fluorescence transient. In *Chlorophyll a Fluorescence: A Signature of Photosynthesis*; Papageorgiou, G.C., Govindjee, Eds.; Springer: Dordrecht, The Netherlands, 2004; pp. 321–362. [CrossRef]

46. R Core Team. *R: A Language and Environment for Statistical Computing*; R Foundation for Statistical Computing: Vienna, Austria, 2021.

47. Lilliefors, H.W. On the Kolmogorov-Smirnov test for normality with mean and variance unknown. *J. Am. Stat. Assoc.* **1967**, *62*, 399–402. [CrossRef]

48. Shapiro, S.S.; Wilk, M.B. An analysis of variance test for normality (complete samples). *Biometrika* **1965**, *52*, 591–611. [CrossRef]

49. Brown, M.B.; Forsythe, A.B. Robust tests for the equality of variances. *J. Am. Stat. Assoc.* **1974**, *69*, 364. [CrossRef]

50. Kruskal, W.H.; Wallis, W.A. Use of ranks in one-criterion variance analysis. *J. Am. Stat. Assoc.* **1952**, *47*, 583–621. [CrossRef]

51. Welch, B.L. On the comparison of several mean values: An alternative approach. *Biometrika* **1951**, *38*, 330–336. [CrossRef]

52. Wilcox, R.R. *Introduction to Robust Estimation and Hypothesis Testing*, 5th ed.; Academic Press: London, UK, 2021.

53. Mond, C.E.D.; Lenth, R.V. A robust confidence interval for location. *Technometrics* **1987**, *29*, 211. [CrossRef]

54. Munns, R.; Tester, M. Mechanisms of salinity tolerance. *Annu. Rev. Plant Biol.* **2008**, *59*, 651–681. [CrossRef] [PubMed]

55. Isayenkov, S.V.; Maathuis, F.J.M. Plant salinity stress: Many unanswered questions remain. *Front. Plant Sci.* **2019**, *10*, 80. [CrossRef]

56. Parihar, P.; Singh, S.; Singh, R.; Singh, V.P.; Prasad, S.M. Effect of salinity stress on plants and its tolerance strategies: A review. *Environ. Sci. Pollut. Res.* **2014**, *22*, 4056–4075. [CrossRef] [PubMed]

57. Zhang, J.-L.; Flowers, T.J.; Wang, S.-M. Mechanisms of sodium uptake by roots of higher plants. *Plant Soil* **2009**, *326*, 45–60. [CrossRef]

58. Kalaji, H.M.; Jajoo, A.; Oukarroum, A.; Brestic, M.; Zivcak, M.; Samborska, I.A.; Cetner, M.D.; Łukasik, I.; Goltsev, V.; Ladle, R.J. Chlorophyll a fluorescence as a tool to monitor physiological status of plants under abiotic stress conditions. *Acta Physiol. Plant.* **2016**, *38*, 102. [CrossRef]

59. Baker, N.R. Chlorophyll fluorescence: A probe of photosynthesis in vivo. *Annu. Rev. Plant Biol.* **2008**, *59*, 89–113. [CrossRef]

60. Murchie, E.H.; Lawson, T. Chlorophyll fluorescence analysis: A guide to good practice and understanding some new applications. *J. Exp. Bot.* **2013**, *64*, 3983–3998. [CrossRef] [PubMed]

61. Lu, C. Salinity treatment shows no effects on photosystem II photochemistry, but increases the resistance of photosystem II to heat stress in halophyte *Suaeda salsa*. *J. Exp. Bot.* **2003**, *54*, 851–860. [CrossRef] [PubMed]

62. Catoni, R.; Gratani, L.; Bracco, F.; Granata, M.U. How water supply during leaf development drives water stress response in *Corylus avellana* saplings. *Sci. Hortic.* **2017**, *214*, 122–132. [CrossRef]

63. Jajoo, A. Changes in photosystem II in response to salt stress. In *Ecophysiology and Responses of Plants Under Salt Stress*; Ahmad, P., Azooz, M.M., Prasad, M.N.V., Eds.; Springer: New York, NY, USA, 2013; pp. 149–168. [CrossRef]

64. Shani, U.; Ben-Gal, A. Long-term response of grapevines to salinity: Osmotic effects and ion toxicity. *Am. J. Enol. Vitic.* **2005**, *56*, 148. [CrossRef]

65. Manishankar, P.; Wang, N.; Köster, P.; Alatar, A.A.; Kudla, J. Calcium signaling during salt stress and in the regulation of ion homeostasis. *J. Exp. Bot.* **2018**, *69*, 4215–4226. [CrossRef] [PubMed]

66. Tavakkoli, E.; Rengasamy, P.; McDonald, G.K. High concentrations of Na^+ and Cl^- ions in soil solution have simultaneous detrimental effects on growth of faba bean under salinity stress. *J. Exp. Bot.* **2010**, *61*, 4449–4459. [CrossRef]

67. Lupo, Y.; Schlisser, A.; Dong, S.; Rachmilevitch, S.; Fait, A.; Lazarovitch, N. Root system response to salt stress in grapevines (*Vitis* spp.): A link between root structure and salt exclusion. *Plant Sci.* **2022**, *325*, 111460. [CrossRef]

68. Gilliham, M.; Dayod, M.; Hocking, B.J.; Xu, B.; Conn, S.J.; Kaiser, B.N.; Leigh, R.A.; Tyerman, S.D. Calcium delivery and storage in plant leaves: Exploring the link with water flow. *J. Exp. Bot.* **2011**, *62*, 2233–2250. [CrossRef] [PubMed]

69. Rengel, Z. The role of calcium in salt toxicity. *Plant Cell Environ.* **1992**, *15*, 625–632. [CrossRef]

70. Mansour, M.M.F. Role of vacuolar membrane transport systems in plant salinity tolerance. *J. Plant Growth Regul.* **2022**, *42*, 1364–1401. [CrossRef]

71. Shabala, S.; Pottosin, I. Regulation of potassium transport in plants under hostile conditions: Implications for abiotic and biotic stress tolerance. *Physiol. Plant.* **2014**, *151*, 257–279. [CrossRef] [PubMed]

72. Storey, R.; Schachtman, D.P.; Thomas, M.R. Root structure and cellular chloride, sodium and potassium distribution in salinized grapevines. *Plant Cell Environ.* **2003**, *26*, 789–800. [CrossRef]

73. Kant, S.; Kafkafi, U.; Pasricha, N.; Bansal, S. Potassium and abiotic stresses in plants. In *Potassium for Sustainable Crop Production*; Johnston, A.E., Ed.; Potash Institute of India: Gurgaon, India, 2002; pp. 233–251.

74. Shabala, S.; Cuin, T.A. Potassium transport and plant salt tolerance. *Physiol. Plant.* **2008**, *133*, 651–669. [CrossRef]

75. Tregeagle, J.M.; Tisdall, J.M.; Tester, M.; Walker, R.R. Cl^- uptake, transport and accumulation in grapevine rootstocks of differing capacity for Cl^--exclusion. *Funct. Plant Biol.* **2010**, *37*, 665–673. [CrossRef]

76. Rahneshan, Z.; Nasibi, F.; Moghadam, A.A. Effects of salinity stress on some growth, physiological, biochemical parameters and nutrients in two pistachio (*Pistacia vera* L.) rootstocks. *J. Plant Interact.* **2018**, *13*, 73–82. [CrossRef]

77. Negrão, S.; Schmöckel, S.M.; Tester, M. Evaluating physiological responses of plants to salinity stress. *Ann. Bot.* **2017**, *119*, 1–11. [CrossRef] [PubMed]

78. Parida, A.K.; Das, A.B. Salt tolerance and salinity effects on plants: A review. *Ecotoxicol. Environ. Saf.* **2005**, *60*, 324–349. [CrossRef] [PubMed]

79. Trapp, S.; Feificova, D.; Rasmussen, N.F.; Bauer-Gottwein, P. Plant uptake of NaCl in relation to enzyme kinetics and toxic effects. *Environ. Exp. Bot.* **2008**, *64*, 1–7. [CrossRef]